



RESEARCH PAPER



TRIM71 binds to IMP1 and is capable of positive and negative regulation of target RNAs

Daniel J. Foster ^a, Hao-Ming Chang^b, Jeffrey R. Haswell^a, Richard I. Gregory^{b,c}, and Frank J. Slack ^a

^aHMS Initiative for RNA Medicine, Department of Pathology, Beth Israel Deaconess Medical Center, Harvard Medical School, Boston, MA, USA; ^bStem Cell Program, Boston Children's Hospital, Department of Biological Chemistry and Molecular Pharmacology, Harvard Medical School, Harvard Stem Cell Institute, Boston, MA, USA; ^cDepartment of Pediatrics, HMS Initiative for RNA Medicine, Harvard Medical School, Boston, MA, USA

ABSTRACT

TRIM71 is an important RNA-binding protein in development and disease, yet its direct targets have not been investigated globally. Here we describe a number of disease and developmentally-relevant TRIM71 RNA targets such as the *MBNL* family, *LIN28B*, *MDM2*, and *TCF7L2*. We describe a new role for TRIM71 as capable of positive or negative RNA regulation depending on the RNA target. We found that TRIM71 co-precipitated with IMP1 which could explain its multiple mechanisms of RNA regulation, as IMP1 is typically thought to stabilize RNAs. Deletion of the NHL domain of TRIM71 impacted its ability to bind to RNA and RNAs bound by congenital hydrocephalus-associated point mutations in the RNA-binding NHL domain of TRIM71 clustered closely with RNAs bound by the NHL deletion mutant. Our work expands the possible mechanisms by which TRIM71 may regulate RNAs and elucidates further potential RNA targets.

ARTICLE HISTORY

Received 22 June 2020
Revised 13 July 2020
Accepted 16 July 2020

KEYWORDS

TRIM71; IGF2BP1; IMP1; crosslinking; RIP-seq; RNABP; liver cancer

Introduction

TRIM71, the human homologue of *C. elegans lin-41*, and a target of the *let-7* microRNA, is highly expressed in early development and decreases in expression as cells differentiate in response to *let-7* increase [1,2]. *TRIM71* is a pluripotency factor that promotes stemness when over-expressed in differentiated cells [3,4] and is essential for mouse development [5]. Knock-out mice die between E8.5–16.5 and have a severe neural tube closure defect [5,6]. *Trim71*^{-/-} mouse ES cells show enrichment of the neuronal development program [7], suggesting that TRIM71 plays a role in inhibiting neuronal development during early embryogenesis. Mutant variants of *TRIM71* have recently been linked to congenital hydrocephalus in patients [8].

TRIM71 is both a ubiquitin ligase and an RNA-binding protein [3,9]. In stem cells, TRIM71 can inhibit translation of the pro-differentiation transcription factor *EGR1* in order to prevent differentiation [4] and can inhibit translation of the cell cycle inhibitor *CDKN1A* [3,10]. For this role, the

ubiquitin ligase activity of TRIM71 is dispensable, as mutating the ubiquitin ligase domain does not impact mRNA binding or mRNA inhibition [3]. Mutations causing phenotypic changes are most frequently localized in the RNA-binding NHL-domain [2,8,11] suggesting that RNA binding is the predominant function of TRIM71.

To understand the role of TRIM71, here we performed a TRIM71 IP-MS, finding co-precipitation with IMP1 (IGF2BP1) and other members of the RNA-stabilizing coding-region instability determinant (CRD) complex. We performed CL-RIP-seq (Crosslinked RNA Immunoprecipitation) and found that 30% of the direct TRIM71 RNA targets are shared with IMP1. The CRD complex is canonically known to stabilize bound RNAs, a notable target being *MYC* [12–15]. IMP1 also plays an important role in development, is a target of *let-7*, and is expressed in early developmental cell fates [12,16,17].

Given the importance of TRIM71 in development, we also studied its role in disease. Hepatocellular carcinoma patients with high levels

CONTACT Frank J. Slack  fslack@bidmc.harvard.edu

 Supplemental data for this article can be accessed [here](#).

© 2020 Informa UK Limited, trading as Taylor & Francis Group

of *TRIM71* have a worse prognosis and depletion of *TRIM71* caused decreased cell proliferation *in vitro* and smaller tumor size in a xenograft model [18]. Conversely, over-expression of *TRIM71* causes larger tumor size in NOD/SCID mice and increased cell proliferation *in vitro* [18]. To better understand the role of *TRIM71* in cancer, we looked more carefully at liver cancer associations and cell phenotypes.

Results

TRIM71 binds to CRD complex members

To determine binding partners of *TRIM71*, we performed an immunoprecipitation (IP) followed by mass spectrometry (MS) in physiologically relevant mouse ES cells [3] and analyzed the peptides using Gene Ontology (GO) analysis (Suppl. Table 1, Suppl. Figures S1, 2). The top GO category was CRD mediated mRNA stabilization. The Coding-Region Instability Determinant (CRD) is an element within mRNAs such as *MYC* that the CRD complex binds to promote mRNA stabilization. This complex is thought to be composed of IMP1 (IGF2BP1), HNRNPU, SYNCRIP, YBX1, and DHX9. The GO category “Regulatory Region RNA Binding” was also enriched and included proteins DHX9, HNRNPA2B1, and PTBP1 (Suppl. Figure S2b).

We followed up on CRD complex members since it was the top GO enriched complex from the IP-MS. We found that *TRIM71* immunoprecipitated with IMP1 and vice versa in HepG2 cells grown in the presence of 4-SU, a photoactivatable ribonucleotide (PAR), and immunoprecipitated, regardless of whether the lysate was treated with RNase (Figure 1(a)). *TRIM71* and IMP1 were also able to immunoprecipitate DHX9 in an RNA-independent manner. Neither *TRIM71* nor IMP1 immunoprecipitated HNRNPU despite it being expressed, so it may not play a role in the CRD complex in these cells. Previously, IMP1 and DHX9 were shown to be dependent on RNA in immunoprecipitation experiments [15], however our experiments were performed in RNA-crosslinked cells which could account for

stronger RNA-mediated protein-protein interactions, which is not disrupted by or perhaps not accessible to RNase. Thus, it is possible that these protein-protein interactions could be RNA-dependent in non-crosslinked conditions.

Next, we tested which *TRIM71* domains were important for IMP1 and DHX9 binding by performing a crosslinked IP (CLIP) on different domain deletion mutants obtained from Worringer et al. (Figure 1(b,c)). Deletion of the coiled-coil domain reduces the interaction with DHX9. Deletions of the NHL, coiled-coil, RING, B-box, or filamin, as well as missense mutations within the RING domain, did not prevent the interaction between *TRIM71* and IMP1 (Figure 1(c)). The NHL domain on its own, which contains no known protein-binding domains, was not able to interact with IMP1 or DHX9 (Figure 1(c)). This suggests that several *TRIM71* domains could be important for the interaction with IMP1 and DHX9, however we were not able to narrow down which might be most important. It is also possible that other proteins may bridge the interaction between *TRIM71* and IMP1 or DHX9. *TRIM71* bound several members of the CRD complex but the NHL domain on its own did not (Figure 1(d)).

TRIM71 CLIP sequencing reveals novel RNA targets

TRIM71 had previously been shown to control cellular growth of hepatocellular carcinoma cells [18]. To better understand the role of *TRIM71* we performed a crosslinked RNA-immunoprecipitation (CL-RIP) followed by sequencing to identify RNA targets in HepG2 cells. This differs from a traditional CLIP in that our samples were not treated with RNase and therefore we could not identify a *TRIM71* binding motif since entire RNAs were eluted rather than short sequences. Replicates of IP and input samples were well-correlated (Suppl. Figure S3a-c). To find RNAs enriched in the IP, we performed

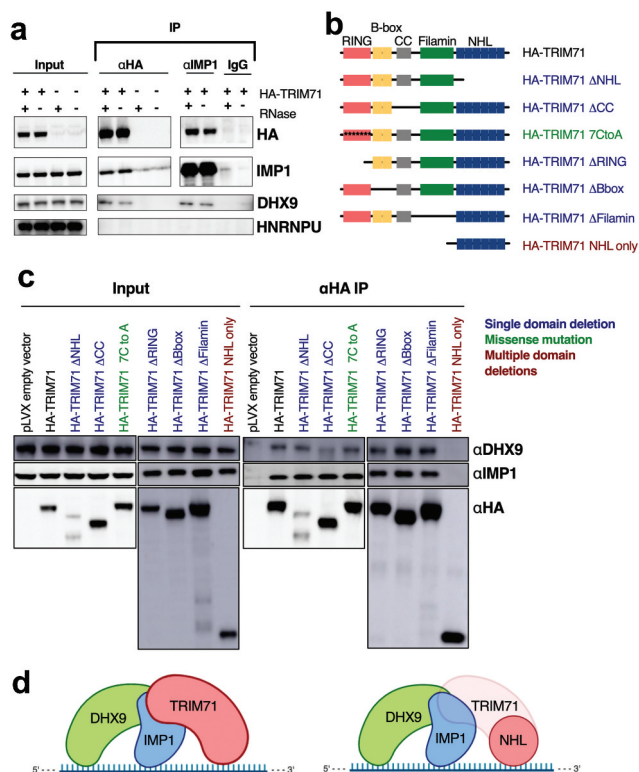


Figure 1. TRIM71 immunoprecipitates with CRD complex members IMP1 and DHX9. (a) TRIM71 immunoprecipitated with CRD complex members IMP1 and DHX9. IMP1 also immunoprecipitated with TRIM71 and DHX9. Neither TRIM71 nor IMP1 co-IP with HNRNPU. The presence of RNase did not impact the ability of any proteins to co-IP each other. (b) TRIM71 domain deletion constructs. No spacers were used in deletion constructs, but are shown for visual ease. (c) Domain deletion IPs were shown to test for domains necessary to co-IP IMP1 and DHX9. No single domain was necessary to bind IMP1 while the coiled-coil domain was necessary to bind DHX9. The NHL-only mutant that lacks all protein binding domains failed to co-IP IMP1 and DHX9. (d) Model of how TRIM71 binds to CRD complex members, left. The NHL domain on its own is unable to bind the CRD complex, right. The translucent portions of TRIM71 represent the domains deleted in part B.

differential expression analysis and found 2,432 RNAs enriched compared to input RNA by greater than a log₂ fold change of 1 and with a false discovery rate (FDR) of <0.05 (Figure 2(a), Suppl. Table 2).

We examined the expression of these genes in a published *Trim71* KO mES cell RNA-seq [7]. Around 80% of our TRIM71 CLIP enriched RNAs were present in the published dataset. Of these, 60% were depleted with *Trim71* KO while 40% were enriched (Suppl. Figure S3e). Thus, although this is a comparison of different cell

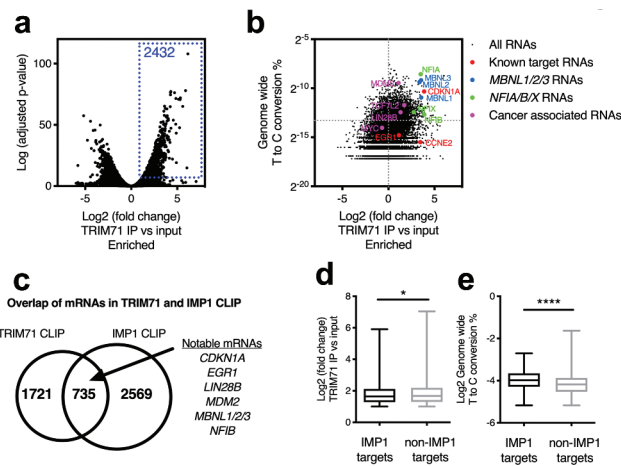


Figure 2. TRIM71 CLIP-sequencing. (a) Differential expression analysis of IP vs Input samples. There were 2432 RNAs significantly enriched with greater than a log₂ fold change of 1 in the IP samples compared to the input (shown in the blue box). These also have expression values greater than a base mean of 15. (b) T to C conversion % per gene is higher in IP enriched genes. Colored dots represent shown genes followed up on with CLIPqPCR. Genes above the horizontal gray dotted line represent genes in the 90th percentile of transitions. (c) Of the 2432 TRIM71-bound RNAs, 30% of them were also bound by IMP1 based on the published IMP1 CLIP dataset from 12. (d) TRIM71 target RNAs also bound by IMP1 were slightly less enriched than non-IMP1 target RNAs. *t*-test *p* = 0.037. (e) IMP1 target RNAs represented a larger % of T to C transition than non-IMP1 targets. *t*-test *p* < 0.0001.

lines, it seems possible that TRIM71 could negatively or positively regulate these RNA target genes.

Prior to crosslinking, the cells were grown in the presence of 4-SU, a photoactivatable ribonucleotide (PAR), to increase crosslinking efficiency. PAR causes predictable thymine to cytosine (T to C) or adenine to guanosine (A to G) transitions where a protein is bound to the RNA. The presence of these transitions is enriched in RNAs that are bound by the protein of interest in an immunoprecipitation experiment. Given that RNA-immunoprecipitation experiments can frequently pull down nonspecific or non-physiologically relevant RNAs, we compared the enriched RNAs against the de-enriched RNAs for the presence of these characteristic transitions. Importantly, we saw more of these transitions in the RNAs enriched in the TRIM71 IP as shown by a rightward shift in the distribution indicating that the CL-RIP enriched RNAs were more likely bound by TRIM71 or protein binding partners of

TRIM71 that are maintained through the harsh wash conditions (Figure 2(b), Suppl. Figure S3g). We mapped the location of all T to C and A to G transitions in the dataset and ranked genes based on the fraction of total transitions in the dataset that each gene contains. In this way, we saw that the top 10% of genes ranked by conversion fraction represent 68% of all T to C or A to G transitions in the dataset. Despite the increase in transitions within the enriched genes, we were unfortunately not able to sufficiently narrow the locations of transitions in the RNA to identify a TRIM71 binding motif, given that the samples were not treated with RNase.

To validate the CL-RIP we looked for known TRIM71 targets *CDKN1A*, *EGR1*, *CCNE2*, and *MBNL1* in our dataset [3,4,19,20]. All four genes were enriched in the CL-RIP samples (Suppl. Figure S4a). *CDKN1A* had many T to C transitions and was in the 99th percentile of genes ranked by conversion fraction. *EGR1* and *CCNE* did not contain many T to C or A to G transitions, likely because they were poorly expressed in these cells (Figure 2(b), lower red points). We also found not only *MBNL1* but the entire *MBNL* family within the 99th percentile of genes ranked by conversion fraction. For consideration of TRIM71 bound RNAs, we focused our attention on genes that were enriched in the IP by >Log₂ fold change of 1, with a FDR <0.05, and within the 90th percentile of genes ranked by conversion fraction. 758 of the 2342 genes enriched in the CL-RIP were within the 90th percentile of genes ranked by conversion fraction. These genes represent potential TRIM71 target RNAs. In addition to finding all members of the muscleblind-like (*MBNL*) family, we found three members of the nuclear factor one (*NFI*) family *NFIA/B/X* (Figure 2(b), blue and green points, Suppl. Fig. S4B). In addition, we also found several liver cancer-associated genes such as *MDM2* and *TCF7L2* enriched in the CLIP and enriched for transitions (Figure 2(b), magenta points, Suppl. Figure S4c).

Given that TRIM71 may bind to IMP1 and CRD complex members, we looked for overlap of bound RNAs to understand whether TRIM71 and IMP1 shared RNA targets. Nearly 30% of the

TRIM71 enriched RNAs were also enriched in published IMP1 CLIP studies (Figure 2(c)) [12,21]. Known IMP1 target *MYC* was within the 80th percentile of genes enriched in transitions but it was actually de-enriched in the IP fraction (Figure 2(b), lower-left magenta dot). Another IMP1 target RNA, *LIN28B*, was relatively enriched in the CLIP and was within the 98th percentile of genes with transitions.

Looking globally at IMP1 bound RNAs in the TRIM71 CL-RIP, these were actually slightly less enriched than the non-IMP1 bound RNAs (Figure 2(d)). Despite the decreased enrichment of the IMP-1 bound RNAs, they represented a higher percentage of T to C transitions in the dataset (Figure 2(e)). The interpretation of this analysis is limited by the fact that Conway, et al. used a different cell line and a different CLIP protocol from ours. Therefore, from this we are not able to determine whether the TRIM71-IMP1 protein interaction impacts RNA binding of TRIM71.

Previous work has shown that TRIM71 may play a role in regulating RNAs that are themselves regulated by miRNAs [3]. To look for miRNA binding motifs we performed Gene Set Enrichment Analysis (GSEA) and found that miRNA targets were highly enriched in the CLIP samples. GSEA for 215 miRNA motifs revealed significant enrichment for 80 miRNA seed motifs in IP versus input analysis whereas only 1 miRNA motif was significantly enriched in the input (Suppl. Figure S5a). Enriched motifs include the miR-302 family, which we previously showed cooperate with TRIM71 silencing of target RNAs [3] (Suppl. Figure S5b). miR-302b/c star motifs were also enriched in the TRIM71 target RNAs (Suppl. Figure S5b). In addition, mRNA targets of several cancer associated miRNAs, miR-21, miR-155, and miR-200a, were enriched (Suppl. Figure S5c).

CLIP sequencing of TRIM71 mutants

We also performed CL-RIP-seq on an NHL-only truncation mutant of TRIM71. Since the NHL domain on its own does not bind CRD complex members (Figure 1(c)), this tested whether

TRIM71 protein binding partners influenced the profile of bound RNAs. Additionally, the NHL domain is thought to provide the RNA target specificity of TRIM-NHL proteins [19], so we wanted to understand the autogenous binding abilities of TRIM71.

We calculated the enrichment of RNA in the NHL-only IP by normalizing to the input in order to account for expression differences between samples that may be caused by overexpressing the TRIM71 constructs. After normalizing the IP samples to input we compared TRIM71 and NHL-only and found that there was a weak correlation between bound RNAs (Suppl. Figure S6a). A correlation matrix of samples also showed that the IP samples of TRIM71 and NHL-only cluster closely together (Suppl. Figure S7b). Despite this, the RNAs bound are not entirely similar, as there are 1679 RNAs enriched in NHL only that were not enriched in TRIM71. This apparent loss of target specificity by NHL-only binding needs to be investigated further.

We calculated a fold change difference score for each gene by taking the difference of the NHL and full-length TRIM71 CLIP enrichments and found that a majority of genes were more highly enriched in the NHL CLIP (Figure 3(a)). Furthermore, 1679 RNAs depleted in full-length TRIM71 CLIP were actually enriched in the NHL CLIP (Suppl. Figure S6a, magenta box). These 1679 RNAs represented a higher percentage of T to C transitions in the NHL CLIP compared to the full-length CLIP suggesting they were true targets of the NHL domain (Figure 3(b), left). Interestingly, the 2432 TRIM71 target RNAs from Figure 2(a) represented fewer T to C conversions in the NHL versus full-length TRIM71 CLIP (Figure 3(b), right).

We performed a CL-RIP-seq on a Δ NHL TRIM71 truncation mutant to understand how RNA binding might be impacted. Similar to previous studies showing that the NHL domain provides RNA specificity [22], deleting the RNA-binding domain of TRIM71 seemed to decrease its ability to bind target RNAs as shown by less enrichment of the 2432 RNAs enriched in full-length TRIM71 (Figure 3(c)). Fold change differences revealed that a vast majority of these RNAs

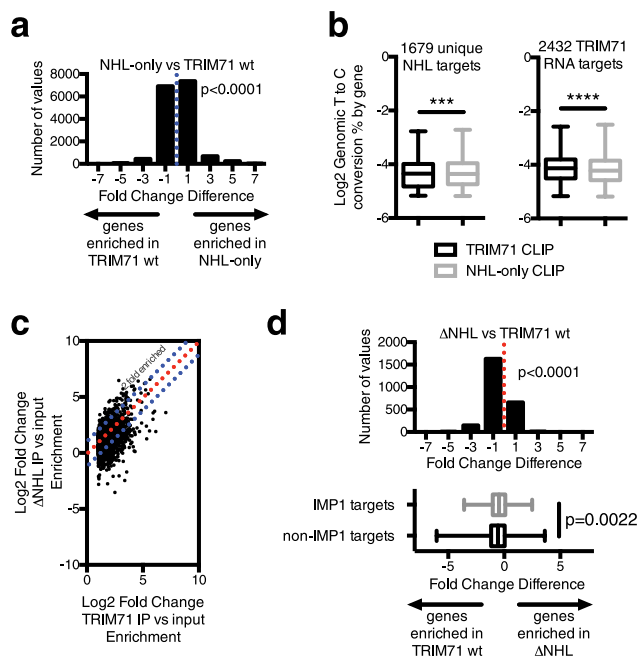


Figure 3. TRIM71 mutant CLIP. (a) Histogram representation of fold change differences calculated by taking the difference between the NHL-only enrichment and full-length TRIM71 enrichment. The histogram distribution is significantly shifted from zero in the direction of enriched in NHL-only, one sample *t*-test. (b) Left, T to C conversion fractions of the 1679 genes bound by NHL but not by TRIM71 show more conversions in the NHL CLIP versus the TRIM71 CLIP, indicating a true hit. Paired *t*-test, $p = 0.0001$. Right, T to C conversion fractions of the 2432 TRIM71 hits showed fewer conversions in the NHL CLIP versus the TRIM71 CLIP indicating less binding to targets. Paired *t*-test, $p < 0.0001$. (c) Differential expression scores of TRIM71 CLIP plotted against enrichment in Δ NHL CLIP. (d) Top, fold change differences show that genes are significantly less enriched in Δ NHL compared to full-length TRIM71, one sample *t*-test. Bottom, fold change differences of IMP1 vs non-IMP1 target RNAs showed that IMP1 targets were significantly more bound than non-IMP1 targets in the Δ NHL CLIP, Welsh's *t*-test.

were less enriched in the Δ NHL mutant (Figure 3(d), top). Interestingly, after separating the target RNAs into IMP1 and non-IMP1 targets, the IMP1 targets were less depleted (Figure 3(d), bottom). We previously showed that the Δ NHL TRIM71 mutant was still able to bind to CRD complex members (Figure 1(c)). Therefore, the relatively stronger enrichment of the Δ NHL TRIM71 truncation mutant with known IMP1 RNA targets suggests that the interaction between TRIM71 and IMP1 may still allow a Δ NHL mutant to bind to RNAs. However, the effect size is small and should be investigated further to fully understand how the interaction between TRIM71 and IMP1 impacts RNA-binding. We confirmed via

CLIP-qPCR that target RNAs of TRIM71 were depleted in the Δ NHL CLIP whereas non-targets were less depleted (Suppl. Figure S6b).

Next, we performed a CL-RIP seq. of NHL missense point mutants that are associated with congenital hydrocephalus [8] (Suppl Figure S7a). Global analysis of bound RNAs revealed that the NHL point mutants cluster closely with the Δ NHL mutants suggesting that these mutations may act as loss of function (Suppl. Figure S7b). It was previously shown that these specific mutations do in fact prevent TRIM71 from regulating a luciferase reporter [22], so we tested which RNA targets were directly impacted in their binding. We compared binding to the 2432 full-length TRIM71 enriched RNAs and found that most are still enriched in the mutant IP samples (Suppl. Figure S7c). However, fold change differences indicate that these mutants were significantly less enriched for the 2432 target RNAs compared to full-length TRIM71 (Suppl. Figure S7d).

Regulation of TRIM71 RNA targets

Via CLIP-qPCR we confirmed that *CDKN1A*, *MBNL1/2/3*, *NFIA/X* and *LIN28B* were significantly enriched in a TRIM71 CL-RIP whereas *ACTIN* and *GAPDH* were not significantly enriched. We also showed binding to cancer-associated genes *MDM2* and *TCF7L2* that were RNA hits in the CL-RIP (Figure 4(a)). We were not able to confirm *EGR1* or *NFIB* binding in HepG2 cells due to the low expression of these genes. Interestingly, despite not being enriched in the CL-RIP seq, *MYC* was significantly enriched when we performed the analysis by qRT-PCR. It is possible that *MYC* is weakly bound by TRIM71 due to its interaction with IMP1, a known *MYC* binding protein. IMP1 could also act as a bridge between TRIM71 and the *MYC* RNA.

Next, we tested the effect of *TRIM71* knock-down on target mRNAs. Upon depletion of *TRIM71* using siRNAs, we saw increased protein levels of p21(*CDKN1A*) and *EGR1*, confirming that TRIM71 was able to negatively regulate these known targets, either through RNA destabilization or translational processes (Figure 4(d), Suppl.

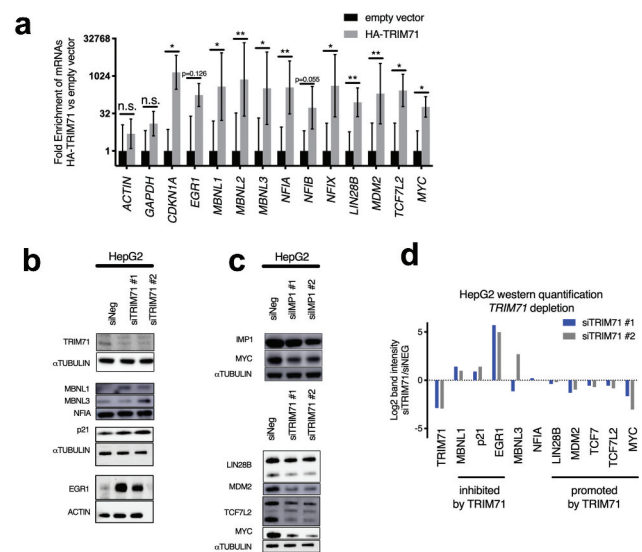


Figure 4. CL-RIP-qPCR and western blot of TRIM71 RNA targets. (a) Fold enrichment of mRNAs in CLIP of cells expressing *HA-TRIM71* versus empty vector control. Known TRIM71 target *CDKN1A* and novel targets *MBNL1/2/3*, *NFIA/X*, *LIN28B*, *MDM2*, *TCF7L2*, and *MYC* were significantly enriched in the TRIM71 CLIP whereas control genes *ACTIN* and *GAPDH* were not. *EGR1* and *NFIB* were not significantly enriched with a p-value of 0.126 and 0.055, respectively. (b) Known TRIM71 targets p21(*CDKN1A*) and *EGR1* were negatively regulated by TRIM71 and knockdown of *TRIM71* increased their expression at the protein level. Novel targets *MBNL1/3* were also increased with *TRIM71* knockdown. *NFIA* was not affected. (c) Knocking down *IMP1* decreased levels of *MYC*. Likewise, knockdown of *TRIM71* also decreased levels of *MYC* indicating TRIM71 positively regulates it. *LIN28B*, *MDM2*, *TCF7*, and *TCF7L2* are also decreased upon *TRIM71* knockdown. (d) Western quantification of target proteins. Signal of blots from (b, c) with TRIM71 depletion were quantified then normalized to the loading control. It was normalized again to siNEG and log2 differences were plotted. Positive values indicate increase levels with TRIM71 depletion whereas negative values indicate decreased levels.

Figure S8a-c). Next we looked at potential novel TRIM71 targets. Consistent with literature [20], we saw slight negative regulation of *MBNL1* with both siRNAs against *TRIM71*. *MBNL3* was affected by one siRNA but not the other. However, *MBNL3* is poorly expressed in HepG2 cells so they are not a good model to understand its function or regulation. We did not see a change in the protein levels of *NFIA* (Figure 4(d), Suppl. Figure S8a). Interestingly, with the other novel targets such as *LIN28B*, *TCF7L2*, and *MDM2*, *TRIM71* knockdown caused a decrease in their protein levels indicating that TRIM71 may be positively regulating these RNAs (Figure 4(e)). TRIM71 knockdown also decreased the protein

levels of the IMP1 target *MYC*. It is unclear whether TRIM71 is interacting directly or indirectly with *MYC*, however, even an indirect interaction through IMP1 would indicate a potential novel mechanism of TRIM71 in regulating RNAs. In HepG2 cells, IMP1 depletion does not seem to have a strong effect on *MYC* protein levels (Figure 4(e) top). Thus, it is possible that the regulation of *MYC* by IMP1 is not very robust in these cells. Therefore, further studies are needed to understand any impact TRIM71 may have on *MYC*, in combination with IMP1 in a more physiologically relevant context.

At the RNA level, TRIM71 depletion decreased levels of *MDM2* and *LIN28B* but not *MYC* (Figure 5(a)). This suggests that TRIM71 is capable of positively regulating potential RNA targets *LIN28B* and *MDM2*. The lack of an effect on *MYC* mRNA but the effect on the *MYC* protein indicates a more complicated and not entirely clear mechanism of regulation.

To confirm that the effect on *LIN28* was due to direct binding of TRIM71 to RNA rather than

a transcriptional effect, we cloned the 3'UTR of *LIN28B* into a dual luciferase reporter and observed that *TRIM71* knockdown decreased reporter activity (Figure 5(b)). This suggests that TRIM71 is capable of binding within this region and promoting stability or translation of the transcript, ruling out a transcriptional effect. Finally, since *LIN28B* is a *let-7* target, we tested if *TRIM71* depletion caused any change in *let-7* levels or activity and found that they were not significantly changed (Figure 5(c,d)). Therefore, it seems unlikely that any regulation of *LIN28B* RNA by TRIM71 is dependent on *let-7*.

Our conclusions surrounding these potentially novel RNA targets of TRIM71 are limited since these experiments were carried out in HepG2 cells. Further analysis in other cell types is warranted to understand whether TRIM71 regulates these RNAs in other physiologically relevant cells.

TRIM71 knockdown slows growth of liver cancer cell lines and induces senescence

TRIM71 is regulated by LIN28A/B and *let-7*, which have both been shown to play a role in oncogenesis [23–28]. Given the role TRIM71 plays in regulating important cell cycle and cancer related oncogenic RNAs within the cell [3,10,18,29], we wanted to better understand its role in cancer. We focused on liver cancer given the liver cancer-associated RNAs found in the TRIM71 CL-RIP (Figures 2(b) and 4) and because there are already reports of TRIM71 playing a role here [18].

We interrogated the Project Achilles and TCGA databases and found that high *TRIM71* expression is correlated with dependency in cancer cell lines, especially so with liver (Suppl. Figure S9a,b). Expression of *TRIM71* is also higher in liver cancer compared to normal liver (Suppl. Figure S9c). However, *TRIM71* expression did not have a significant effect on patient survival based on median expression of all HCC patients (Suppl. Figure S9d). Interestingly, GSEA revealed that TRIM71 target RNAs were enriched for genes downregulated when *CTNNB1* is overexpressed in cells (Suppl. Figure S9e). *CTNNB1* is

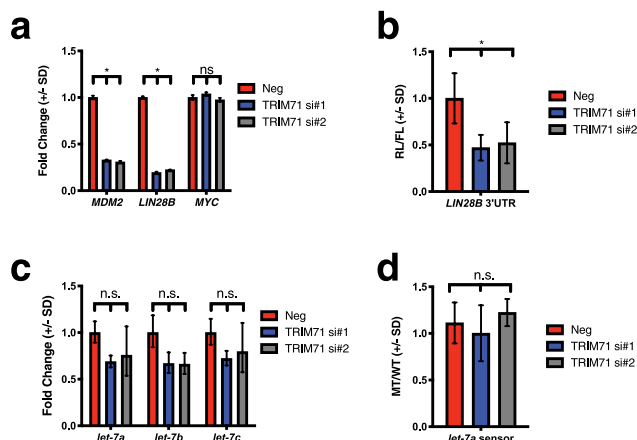


Figure 5. TRIM71 affects mRNA levels of some targets while *let-7* levels and activity are unchanged. (a) *TRIM71* knockdown decreased mRNA levels of *MDM2* and *LIN28B* but not *MYC* in HepG2 cells. Error bars represent S.D. of two (*MDM2*) or three (*LIN28B*, *MYC*) biological replicates, *t*-test $p < 0.05$. (b) A PsiCheck2 luciferase reporter with the *LIN28B* 3'UTR showed decreased activity with *TRIM71* knockdown. Error bars represent S.D. One-way ANOVA, $p < 0.05$. (c) *TRIM71* depletion did not affect *let-7* levels measured by qPCR. One-way ANOVA. (d) A PsiCheck2 *let-7a* sensor was not changed with *TRIM71* knockdown. MT refers to a non-complementary mutant *let-7a* sensor while WT is fully complementary. Not significant based on one-way ANOVA.

a commonly overexpressed oncogene in liver cancer, including HepG2 cells, so it is notable that the TRIM71-bound RNAs are enriched for genes regulated by CTNNB1.

Given the association of *TRIM71* expression with dependency in cell lines, we depleted *TRIM71* with siRNAs in liver cancer cell lines HepG2 and Huh7 (Suppl. Figure S10a) and then performed MTT and BrdU assays to test for growth phenotypes. *TRIM71* knockdown significantly decreased proliferation as measured by MTT of HepG2 and Huh7 cells (Suppl. Figure S10b). BrdU incorporation was significantly decreased in HepG2 (Suppl. Figure S10c). These *TRIM71*-dependent liver cancer growth phenotypes were similar to those seen in previous studies [18]. We did not see suppression of these phenotypes with knockdown of *CDKN1A* (Suppl. Figure S11a,b) [3].

Noting that HepG2 cells treated with *TRIM71* siRNA exhibited a strong morphological change (Suppl. Figure S10d), we tested for senescence by blotting for levels of p16(INK4A) and found increases in HepG2 and Huh7 (Suppl. Figure S10e). Staining for senescence-associated β -glycosidase (SA- β gal) showed a strong induction of senescence in HepG2 (Suppl. Figure S10d,f). We did not observe differences in senescence in Huh7 cells compared to HepG2, as expected, due to mutation of p53 in Huh7 cells. Furthermore, based on GSEA (Suppl. Figure S9e), *TRIM71* RNA targets show enrichment in RNAs changed in *CTNNB1* dependent cells such as HepG2, and not Huh7. Overexpression of *MYC* but not *GFP* rescued the morphological change and partially rescued SA- β gal staining (Suppl. Figure S11c-f).

Discussion

Here we have shown that *TRIM71* is capable of binding to CRD complex member IMP1 and DHX9 in a seemingly RNA-independent manner. Since the CRD complex has been shown to positively regulate the RNAs it binds, these novel interactions suggest that *TRIM71* may be capable of additional molecular mechanisms not previously described. We hypothesized that *TRIM71*

would be capable of positively regulating RNAs, like the CRD complex members to which it binds.

To determine the RNAs bound by *TRIM71* we performed a CL-RIP-seq, finding previously described RNAs as bound, such as *CDKN1A* and *MBNL1*. Furthermore, we found miRNA-targeted mRNAs were significantly enriched in the *TRIM71* CLIP-seq. Including mRNA targets of the miR-302 family. *MBNL1* was recently described as a target mRNA of *TRIM71* [20]. Here we show that all three *MBNL* family members may be *TRIM71* targets as well as 3 of 4 *NFI* family members. We show that *TRIM71* seems to be inhibiting *MBNL1* but we were not able to show a conclusive effect on *MBNL3* or any effect on expression of the *NFI* family members. Lastly, *TRIM71* was bound to *LIN28B*, *MDM2*, and *TCF7L2*, and seemed to positively regulate these RNAs. *LIN28B*, *MDM2*, and *TCF7L2* are important in liver cancer which could further explain the effects of *TRIM71* in liver cancer [18] and the effects we see upon *TRIM71* knockdown in liver cancer cell lines HepG2 and Huh7.

The mechanism by which *TRIM71* potentiates different RNAs may vary, similar to IMP1. For *LIN28B*, there are many miRNA complementary sequences within the 3'UTR. It is possible that the binding of *TRIM71* to *LIN28B* is obstructing miRNA binding and that depletion of *TRIM71* opens these sites up to binding and subsequent inhibition/degradation. IMP1 and IMP2 are able to bind target mRNAs to prevent miRNA silencing in this way [30]. Unfortunately, we were not able to determine binding localization on the RNAs from the CL-RIP since the samples were not treated with RNase. However, we did show that the *TRIM71* target RNAs are enriched in miRNA targets suggesting that *TRIM71* could operate through this mechanism.

Regarding *MYC*, IMP1 is known to bind in the CRD element of the CDS rather than the 3'UTR. IMP1 is capable of regulating RNAs in a multitude of mechanisms and the regulation of *MYC* seems to be that of protection against degradation by nucleases [31–35]. Interestingly, we did not see regulation of the *MYC* mRNA when we depleted *TRIM71* however we saw a decrease in protein

levels. It is possible that TRIM71 does not contribute to mRNA stabilization of *MYC* but rather to the translational process (or protein stability). Other CRD complex members such as HNRNPE and STAU1 also do not directly affect the stability of the *MYC* RNA. Instead TRIM71 may recruit other proteins such as PABPC1, which bound Trim71 in the IP-MS, to facilitate translation. Further studies are needed to elucidate the mechanism of regulation of *MYC* and whether the interaction between TRIM71 and *MYC* is direct or bridged by other proteins.

Next, we wanted to better understand how TRIM71 mutant proteins bind RNA. It has been shown previously that the NHL domain provides specificity to RNA binding [22]. Our results here showing that the Δ NHL mutant binds RNAs less strongly supports that view. Furthermore, we performed a CL-RIP seq of TRIM71 with point mutations within the NHL domain showing that the RNAs bound cluster closely with the Δ NHL mutant, suggesting that these point mutants may act as a loss of function.

The interaction with protein binding partners such as IMP1 may be important for TRIM71 RNA specificity. The interactions between TRIM71 and IMP1 could allow for an additive effect of their RNA-binding domains that together provide greater specificity for binding RNAs. Future studies can investigate this hypothesis by knocking down IMP1 and measuring the RNAs bound by TRIM71.

We have presented here that TRIM71 is able to bind novel RNAs with roles in development, oncogenesis, and the cell cycle. TRIM71 co-precipitates with CRD complex members IMP1 and DHX9. Like IMP1, TRIM71 is capable of regulating different RNAs in a positive and negative manner. Furthermore, the interaction between TRIM71 and IMP1 could be critical for specifying RNAs bound by TRIM71, especially a Δ NHL mutant. If the RNA binding of TRIM71 is influenced by protein binding partners, this opens up the possibility of context-dependent regulation of RNAs by TRIM71 and could partially explain why TRIM71 is positively regulating some RNAs and negatively regulating others.

Materials and methods

Cell culture

HepG2 cells were purchased from the American Type Culture Collections (ATCC). Huh-7 and Huh-6 cells were purchased from the Japanese Collection of Research Bioresources (JCRB) Cell Bank. All cells were cultured in media containing 10% Fetal Bovine Serum (FBS), 100 I.U./mL penicillin, and 100 ug/mL streptomycin unless otherwise noted. Culture conditions: HepG2: Dulbecco's Modified Eagles Medium (DMEM) with 4.5 g/L glucose. Huh-7: DMEM with 1 g/L glucose. Huh6: RPMI with 4% FBS.

Antibodies

Used for western blot: α -Tubulin (#2144), MYC (#5605), LIN28B (#4196), p21 (#2947), EGR1 (#4154), IMP1 (#8482), HA-tag (#3724) from Cell Signaling Technology; LIN-41 (55003-1-AP), p16INK4A (10883-1-AP), NFIA (11750-1-AP), MBNL3 (24610-1-AP) from Proteintech. MBNL1 (sc-47740) from Santa Cruz Biotechnology. Used for IP and cross-linking IP: α -IMP1 (#8482) from Cell Signaling Technology; α -HA-tag (H6908) from Sigma-Aldrich; IgG (I5006).

Western blotting

Cells were lysed in RIPA buffer and incubated on ice for 10 min, vortexing every 2 min. Lysates were centrifuged at 13,200rpm for 20 min. Laemmli buffer was added to the cleared lysates and run in 4–12% NuPAGE gels (Thermo Fisher #NP0316BOX) with corresponding buffer (Thermo Fisher #NP0001). Proteins were transferred to nitrocellulose or PVDF membranes and blocked in 3–5% milk. Primary antibodies were incubated at 4°C overnight. Membranes were washed 3 times with TBST, for 5 min each. HRP-conjugated secondary antibodies (Santa Cruz) were incubated at room temperature for 2 hours at a 1:10,000 dilution. Membranes were washed 3 times with TBST, for 5 min each. Protein was detected using Chemiluminescent substrate (Thermo Fisher #34,580).

Quantification of westerns

Western bands were quantified using ImageStudioLite (Licor version 5.2.5). Test genes were normalized to the loading control by dividing the two signals (Test/Loading Control). This normalized signal was calculated for each treatment conditions (e.g. siNEG, etc.). Next, siRNA treatment conditions were compared by dividing the gene specific siRNA samples by siNEG (e.g. normalized siTRIM71/normalized siNEG).

RNA isolation, cDNA synthesis, RT-qPCR

Cells were lysed in TRIzol reagent and RNA was isolated using the Direct-zol RNA Kit (Zymo). For expression analysis, 1 μ g of total RNA was reverse transcribed using SuperScriptIV (Invitrogen) and primed with 20-mer oligo dT (Integrated DNA Technologies). For CLIP-qPCR, 11 μ L of RNA was added to cDNA reaction and primed with random hexamers. cDNA was diluted 1:5 for qPCR expression analysis using either LightCycler FastStart DNA Master SYBR Green I (Roche) or QuantiTech SYBR Green (Qiagen) in a LightCycler 480 System (Roche).

siRNA transfections

Cells were transfected with ThermoFisher pre-designed Silencer Select siRNA, cat. # 4392420 and 4390843 at a final concentration of 20 nM. siRNA IDs: TRIM71 (s43598, s43599), IGF2BP1 (s20916, s20917), CDKN1A (s416). All siRNA transfections were performed using Lipofectamine RNAiMax #13778150. HepG2 cells were reverse transfected in 6-well plates for 3 days before being split for further cell assays. Huh6 cells were reverse transfected for 3 days and protein lysate was collected without splitting the cells. Huh7 cells were forward transfected for 3 days in 6-well plates before being split for further cell assays.

MTT assay

Cells were seeded for MTT assay on day 4, following the 3-day transfection described above. HepG2 cells were seeded at 1,000 cells/well in a 96-well. Huh7 cells

were seeded at 2,000 cells/well. For each day of the assay, MTT dye was added to the cells, incubated for 2 hours, aspirated, dissolved in 100 μ L DMSO, then the absorbance was read at 565 nm.

BrdU assay

Millipore BrdU Cell Proliferation Assay kit cat. # 2750 was used to detect and measure BrdU incorporation according to manufacturer protocol following the standard 3-day siRNA transfection above.

Luciferase assay

HepG2 cells were transfected with luciferase plasmids, pscheck 2, which had the *LIN28B* 3'UTR or a *let-7* responsive elements cloned behind renilla luciferase. Cells were transfected for 2 days then processed according to the Promega dual-luciferase reporter system protocol.

Plasmids and cloning

HA-TRIM71 pMXs plasmids and deletion mutants were obtained from Addgene (Cat #: 52717, 52718, 52719, 52720, 52721, 52722, 52726). *LIN28B*, *MYC*, and *GFP* pcDNA3 plasmids for overexpression experiments were ordered from Addgene (Cat #: 51373, 74162, 13031, 16233, respectively). *TRIM71* and other overexpression gene sequences were subcloned from pMXs and pcDNA3 plasmids into a puromycin selectable pLVX plasmid (Clontech #632159) for lentiviral based stable transductions. For transductions we used Addgene plasmids psPAX2 (#122560) and pCMV-VSV-G (#8454). For luciferase experiments, the 3'UTR of *LIN28B* was cloned into the pscheck-2 plasmid from Promega. Pscheck-2 *let-7* wt and Pscheck-2 *let-7* mt plasmids were ordered from Addgene (cat # 78260, 78261).

Trim71 IP-MS

KH2 ES cell lines [3] were treated with Dox at 1 μ g ml⁻¹ for 72 h then collected in lysis buffer (20 mM Tris-HCl, pH 8.0, 137 mM NaCl, 1 mM EDTA, 1% (v/v) Triton X-100, 10% (v/v) Glycerol,

1.5 mM MgCl₂, 1 mM DTT, 0.2 mM PMSF). Protein complexes were affinity-purified using Flag M2 agarose beads (Sigma) and washed 3X with EDTA-free BC buffer with 100 mM KCl, treated with 20 µg ml⁻¹ of RNase A (in EDTA-free BC-100 buffer) for 30 min at 37°C, and washed 3 more times before elution with 0.5 mg ml⁻¹ Flag peptide.

Cross-linking RNA IP

We used a CLIP protocol modified from Moore, et al. [36]. HepG2 cells were incubated for 14–18 hours in media supplemented with 4-SU at a final concentration of 100µM. Cells were cross-linked for 72 seconds with a Stratalinker 1800 emitting 3000uL/sec/cm² at 365 nM. Buffers were made according to the Moore, et al.[36] protocol. Cells were lysed according to the Moore, et al. protocol. 100uL of lysate was set aside as IP input control and the rest of the cell lysate was incubated with anti-HA-conjugated Protein G dynabeads [Thermo Fisher #10004D] for 2 hours and washes were as follows: 3x washes with PXL buffer, 3x high-salt buffer, 3x washes of high stringency buffer, 3x washes of low salt buffer, 2x washes of PNK buffer. Beads were treated with diluted proteinase K according to Moore, et al.[36]. 600uL of TRIzol was added to cell lysates and RNA was extracted as described above.

Each CLIP sample was sequenced in duplicate. Libraries were made using low input SMARTer V4 for total RNA (Takara #635007) followed by rRNA depletion. Libraries were sequenced using Illumina NextSeq500 with single-end 75bp reads by the Dana Farber Molecular Biology Core Facility. Each sample was sequenced to a depth of ~20 M reads.

Bioinformatic analysis

Reads were aligned to the genome using bowtie and PCR duplicates were flagged and removed using bamsormadup and samtools. Differential expression analysis was performed on 2 replicates for every sample using DEseq2. Genes with fewer

than 15 base-mean reads were excluded from DE analysis. The PAR-CLIP data analyzer [37] was used to calculate T to C and A to G transition fractions for each gene. We calculated the # of total transitions in the dataset and ranked genes by the percentage of transitions that each gene represents as a part of the total. TRIM71 target genes were defined as genes with Log2 foldchange >1, a false discovery rate >0.05, and transition fraction within the top 90th percentile of genes.

Figure 3 and Suppl. Figure S7 were analyzed using the full set of statistically enriched RNAs (2432), rather than narrowing to the RNAs in the top 90th percentile of transitions.

Acknowledgments

We thank members of the Slack Lab for critical reading of this manuscript and Kristopher Kahle for the NHL point-mutant plasmids. We acknowledge the NCI Outstanding Investigator Award (R35CA232105) to FJS and we thank the Ludwig Center at Harvard as well as the National Science Foundation for funding GRFP: DGE1144152 to DJF.

HMC performed the IP-MS. JRH performed RIP-qPCRs. DJF performed all other experiments and with FJS wrote the manuscript. All authors contributed to editing the manuscript.

Disclosure statement

No potential conflict of interest was reported by the authors.

Funding

This work was supported by the National Cancer Institute [R35CA232105].

ORCID

Daniel J. Foster  <http://orcid.org/0000-0002-2466-9484>

Frank J. Slack  <http://orcid.org/0000-0001-8263-0409>

References

- [1] Schulman BR, Esquela-Kerscher A, Slack FJ. Reciprocal expression of lin-41 and the microRNAs let-7 and mir-125 during mouse embryogenesis. *Dev Dyn.* 2005;234:1046–1054.

- [2] Slack FJ, Basson M, Liu Z, et al. The lin-41 RBCC gene acts in the *C. elegans* heterochronic pathway between the let-7 regulatory RNA and the LIN-29 transcription factor. *Mol Cell*. 1999;5:659–669.
- [3] Chang H-M, Martinez NJ, Thornton JE, et al. Trim71 cooperates with microRNAs to repress Cdkn1a expression and promote embryonic stem cell proliferation. *Nat Commun*. 2012;3:923.
- [4] Worringer KA, Rand TA, Hayashi Y, et al. The let-7/LIN-41 pathway regulates reprogramming to human induced pluripotent stem cells by controlling expression of prodifferentiation genes. *Cell Stem Cell*. 2014;14:40–52.
- [5] Schulman BR, Liang X, Stahlhut C, et al. The let-7 microRNA target gene, Mlin41/Trim71 is required for mouse embryonic survival and neural tube closure. *Cell Cycle (Georgetown, Tex)*. 2008;7:3935–3942.
- [6] Chen J, Lai F, Niswander L. The ubiquitin ligase mLin41 temporally promotes neural progenitor cell maintenance through FGF signaling. *Genes Dev*. 2012;26:803–815.
- [7] Mitschka S, Ulas T, Goller T, et al. Co-existence of intact stemness and priming of neural differentiation programs in mES cells lacking Trim71. *Sci Rep*. 2015 (5). doi:10.1038/srep11126.
- [8] Furey CG, Choi J, Jin SC, et al. De Novo mutation in genes regulating neural stem cell fate in human congenital hydrocephalus. *Neuron*. 2018;99:302–314.e304.
- [9] Rybak A, Fuchs H, Hadian K, et al. The let-7 target gene mouse lin-41 is a stem cell specific E3 ubiquitin ligase for the miRNA pathway protein Ago2. *Nat Cell Biol*. 2009;11:1411–1420.
- [10] Rand TA, Sutou K, Tanabe K, et al. MYC releases early reprogrammed human cells from proliferation pause via retinoblastoma protein inhibition. *Cell Rep*. 2018;23:361–375.
- [11] Slack FJ, Ruvkun G. A novel repeat domain that is often associated with RING finger and B-box motifs. *Trends Biochem Sci*. 1998;23:474–475.
- [12] Conway AE, Van Nostrand EL, Pratt GA, et al. Enhanced CLIP uncovers IMP protein-RNA targets in human pluripotent stem cells important for cell adhesion and survival. *Cell Rep*. 2016;15:666–679.
- [13] Hafner M, Landthaler M, Burger L, et al. Transcriptome-wide identification of RNA-binding protein and microRNA target sites by PAR-CLIP. *Cell*. 2010;141:129–141.
- [14] Van Nostrand EL, Pratt GA, Shishkin AA, et al. Robust transcriptome-wide discovery of RNA-binding protein binding sites with enhanced CLIP (eCLIP). *Nat Methods*. 2016;13:508–514.
- [15] Weidensdorfer D, Stöhr N, Baude A, et al. Control of c-myc mRNA stability by IGF2BP1-associated cytoplasmic RNPs. *RNA*. 2009;15:104–115.
- [16] Degrauwe N, M-L S, Janiszewska M, et al. IMPs: an RNA-binding protein family that provides a link between stem cell maintenance in normal development and cancer. *Genes Dev*. 2016b;30:2459–2474.
- [17] Nishino J, Kim S, Zhu Y, et al. A network of heterochronic genes including Imp1 regulates temporal changes in stem cell properties. *eLife*. 2013;2:e00924.
- [18] Chen YL, Yuan RH, Yang WC, et al. The stem cell E3-ligase Lin-41 promotes liver cancer progression through inhibition of microRNA-mediated gene silencing. *J Pathol*. 2013;229:486–496.
- [19] Loedige I, Gaidatzis D, Sack R, et al. The mammalian TRIM-NHL protein TRIM71/LIN-41 is a repressor of mRNA function. *Nucleic Acids Res*. 2013;41:518–532.
- [20] Welte T, Tuck AC, Papasaikas P, et al. The RNA hairpin binder TRIM71 modulates alternative splicing by repressing MBNL1. *Genes Dev*. 2019;33:1221–1235.
- [21] Müller S, Bley N, Glaß M, et al. IGF2BP1 enhances an aggressive tumor cell phenotype by impairing miRNA-directed downregulation of oncogenic factors. *Nucleic Acids Res*. 2018;46(12):6285–6303.
- [22] Kumari P, Aeschmann F, Gaidatzis D, et al. Evolutionary plasticity of the NHL domain underlies distinct solutions to RNA recognition. *Nat Commun*. 2018;9:1549.
- [23] Gilles M-E, Slack FJ. Let-7 microRNA as a potential therapeutic target with implications for immunotherapy. *Expert Opin Ther Targets*. 2018;22:1–11.
- [24] Johnson CD, Esquela-Kerscher A, Stefani G, et al. The let-7 microRNA represses cell proliferation pathways in human cells. *Cancer Res*. 2007;67:7713–7722.
- [25] Johnson SM, Grosshans H, Shingara J, et al. RAS is regulated by the let-7 MicroRNA family. *Cell*. 2005;120:635–647.
- [26] Thornton JE, Gregory RI. How does Lin28 let-7 control development and disease? *Trends Cell Biol*. 2012;22:474–482.
- [27] Viswanathan SR, Daley GQ. Lin28: a microRNA regulator with a macro role. *Cell*. 2010;140:445–449.
- [28] Viswanathan SR, Powers JT, Einhorn W, et al. Lin28 promotes transformation and is associated with advanced human malignancies. *Nat Genet*. 2009;41:843–848.
- [29] Nguyen LH, Robinton DA, Seligson MT, et al. Lin28b is sufficient to drive liver cancer and necessary for its maintenance in murine models. *Cancer Cell*. 2014;26:248–261.
- [30] Degrauwe N, Schlumpf TB, Janiszewska M, et al. The RNA binding protein IMP2 preserves glioblastoma stem cells by preventing let-7 target gene silencing. *Cell Rep*. 2016;15:1634–1647.
- [31] Bernstein PL, Herrick DJ, Prokipcak RD, et al. Control of c-myc mRNA half-life in vitro by a protein capable

- of binding to a coding region stability determinant. *Genes Dev.* [1992](#);6:642–654.
- [32] Doyle GAR, Leeds PF, Fleisig AJ. The c-myc coding region determinant-binding protein: a member of a family of KH domain RNA-binding proteins. *Nucleic Acids Res.* [1998](#);26(22):5036–5044.
- [33] Huang H, Weng H, Sun W, et al. Recognition of RNA N6-methyladenosine by IGF2BP proteins enhances mRNA stability and translation. *Nat Cell Biol.* [2018](#);20:285–295.
- [34] Lemm I, Ross J. Regulation of c-myc mRNA decay by translational pausing in a coding region instability determinant. *Mol Cell Biol.* [2002](#);22(12):3959–3969.
- [35] Sparanese D, Lee CH. CRD-BP shields c-myc and MDR-1 RNA from endonucleolytic attack by a mammalian endoribonuclease. *Nucleic Acids Res.* [2007](#);35:1209–1221.
- [36] Moore MJ, Zhang C, Gantman E, et al. Mapping Argonaute and conventional RNA-binding protein interactions with RNA at single-nucleotide resolution using HITS-CLIP and CIMS analysis. *Nat Protoc.* [2016](#);9:263–293.
- [37] Corcoran DL, Georgiev S, Mukherjee N, et al. PARalyzer: definition of RNA binding sites from PAR-CLIP short-read sequence data. *Genome Biol.* [2011](#);12:R79.